

## INVERSE METHOD FOR TRANSIENT TEMPERATURE ESTIMATION DURING MACHINING

M. LAZARD and P. CORVISIER

*ERMEP, Institut Supérieur d'Ingénierie de la Conception, 27 rue d'Hellieule, 88100 Saint Dié, France*

E-mail: [mlazard@insic.fr](mailto:mlazard@insic.fr)

**Abstract** – We consider the problem of estimating the transient temperature and the heat flux at the tip of a tool during a turning process using an inverse approach. The model of the heat transfer is based on a quadrupole formulation and it is tested on numerical simulations incorporating noise.

### 1. INTRODUCTION

The need for protection and for adaptive control of numerically controlled machine tools against machine breakage and wear has become a priority over the past few years [1, 2, 9, 17]. During the turning process, the damage of the tool insert strongly depends on the temperature [7, 8]. That is the reason why several authors have become interested in determining the temperature [3, 4, 5, 12, 13]: some measure steady-state tool-chip interface temperature with an infrared camera [13], others measure the temperature at the tip of the tool with thermocouples [3, 4, 5] and use a non integer identified model to solve the inverse heat conduction problem [5].

However, it is very arduous to measure experimentally the temperature at the tip. Two major drawbacks can be put forward: in the case of tool's wear, the thermocouple could be damaged and the thermal gradient is very high in this zone, as a consequence, the measurements are not very accurate.

The goal of this paper is to avoid this problem and to propose an accurate measurement methodology using an inverse approach. Hence, two thermocouples are located at two different locations in the insert tool. The heat transfer is then described with a model based on the quadrupole formulation. The transient temperature of the tip is evaluated using the inverse model. Then the results are tested with simulations performed with the numerical code based on the finite volume method Fluent® for different temperatures profiles (Heaviside, exponential solicitations). Moreover, to reproduce experimental conditions, noise is added to the transient temperature.

### 2. DESCRIPTION AND GOVERNING EQUATIONS OF THE THERMAL PROBLEM

In this section, the governing equations are given in cylindrical coordinates and the solution of the thermal equations is expressed in Bessel functions and then with a quadrupole formulation.

#### 2.1 Description

A schematic view of the front of the insert is proposed in the Figure 1. It is composed of a rounded tip (radius  $r_0$ ). Cylindrical surfaces  $S_0, S_1, S_2$  (corresponding to the radii  $r_0, r_1, r_2$ ) are plotted. The heat transfer in the tip of the tool is assumed to be essentially radial. As a consequence the surfaces  $S_0, S_1, S_2$  correspond to isothermal surfaces in the tool insert (this assumption is checked in section 3 using direct numerical simulations with the parameters summarized in the Table 1 and subject to physical considerations).

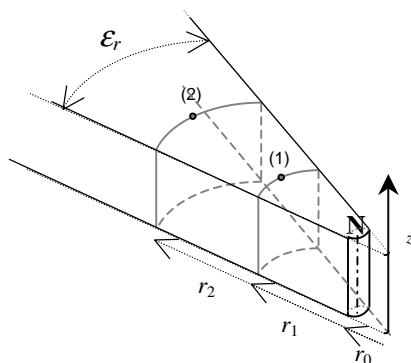


Figure 1 : Geometry of tool insert.

Geometrical parameters				
Radius (mm)			Thickness (mm)	Angle (°)
$r_0 = 1$	$r_1 = 7$	$r_2 = 16$	$e = 4$	$\epsilon_r = 35$

Thermophysical parameters		
Density $kg \cdot m^{-3}$	Calorific capacity $J \cdot kg^{-1} \cdot K^{-1}$	Thermal conductivity $W \cdot m^{-1} \cdot K^{-1}$
$\rho = 19200$	$c_p = 135$	$\lambda = 150$

Table 1 : Parameters used for simulations.

The mechanical energy during the cutting process corresponds to the work due to the engine torque applied on the workpiece. A part of this energy is dissipated as heat between the workpiece and the tool insert. The heat

flux  $\phi$  is composed of three contributions: the heat flux absorbed by the piece  $\phi_m$ , the heat flux convected by the chips  $\phi_c$  and finally the heat flux absorbed by the tool insert  $\phi_N$ .

A heat flux  $\Phi_0$  goes through the surface  $S_0$  for  $r=r_0$  at the temperature  $T_0$  and a heat flux  $\Phi_1$  goes through the surface  $S_1$  for  $r=r_1$  at the temperature  $T_1$ . The point  $N$  is located on the surface  $S_0$  and corresponds to the tip of the insert. The points 1, 2 are located on the isothermal surfaces where the measurements are made. The aim of this work is to provide a good approximation of the temperature of the tip of the tool and the heat flux within the smallest computational time. One knows that this maximum is not exactly located at the tool tip but in a very close region [15, 18]. So, the exact position and value of the temperature maximum is not perfectly determined by this model but conversely the heat flux crossing through the tool insert is well estimated. The measurement is also very sensitive to the precise location of the thermocouples. So, the first thermocouple is fixed near the hottest zone and the second far enough away from it to increase the accuracy of the maximum temperature measurement.

## 2.2 Governing equations in cylindrical coordinates

The heat transfer equations could be written as follow in cylindrical coordinates:

$$\frac{1}{r} \frac{\partial}{\partial r} \left( r \frac{\partial T(r,t)}{\partial r} \right) = \frac{1}{\alpha} \frac{\partial T(r,t)}{\partial t} \quad (1)$$

$$\Phi(r,t) = -\lambda S(r) \frac{\partial T(r,t)}{\partial r} \quad (2)$$

where  $T$  is the temperature,  $r$  is the radial abscissa,  $\alpha$  is the thermal diffusivity,  $t$  is the time,  $\Phi$  is the heat flux,  $\lambda$  is the thermal conductivity and  $S$  is the surface.

The Laplace transform is applied on the temperature and the heat flux to give:

$$\theta(p) = L(T(t) - T_{ext}) = \int_0^{+\infty} (T(t) - T_{ext}) \exp(-pt) dt$$

with  $T_{ext}$  the external temperature and

$$\phi(p) = \int_0^{+\infty} \Phi(t) \exp(-pt) dt .$$

Then, the transformed temperature is found to satisfy the following differential equation:

$$\frac{d^2 \theta}{dr^2} + \frac{1}{r} \frac{d\theta}{dr} - \frac{p}{\alpha} \theta = 0 \quad (3)$$

The solution of these equations is:

$$\theta(r) = c_1 I_0(kr) + c_2 K_0(kr) \quad (4)$$

$$\phi(r) = -\lambda S(r) c_1 k I_1(kr) + \lambda S(r) c_2 k K_1(kr) \quad (5)$$

$$k = \sqrt{\frac{p}{\alpha}} \quad (6)$$

The boundary conditions are:

$$\theta(r_1) = \theta_1 = L(T_1 - T_{ext}) \quad (7a)$$

$$\phi(r_1) = \phi_1 \quad (7b)$$

They permit the calculation of the two constants  $c_1$  and  $c_2$ .

In order to easily determine the temperature and the heat flux at the tip of the tool, a specific method based on the quadrupole formulation is used in the next sections.

## 2.3 Quadrupole formulation

The quadrupole formulation is commonly used to solve ordinary differential equations in the Laplace domain [11, 14, 16]. It provides a transfer matrix for the medium that linearly links the input temperature-heat flux column vector at the front side ( $r = 0$ ) and the output vector at the rear side ( $r = 1$ ).

The quadrupole formulation of equation (3) is:

$$U_0 = \begin{pmatrix} \theta(r_0) \\ \phi(r_0) \end{pmatrix} = \begin{pmatrix} \theta_0 \\ \phi_0 \end{pmatrix} = \begin{pmatrix} A & B \\ C & D \end{pmatrix} \begin{pmatrix} \theta_1 \\ \phi_1 \end{pmatrix} = \begin{pmatrix} A & B \\ C & D \end{pmatrix} \begin{pmatrix} \theta(r_1) \\ \phi(r_1) \end{pmatrix} = MU_1 \quad (8)$$

with

$$A = \lambda k S(r_1) [K_1(kr_1)I_0(kr_0) + I_1(kr_1)K_0(kr_0)] / E \quad (8a)$$

$$B = K_0(kr_0)I_0(kr_1) - I_0(kr_0)K_0(kr_1) / E \quad (8b)$$

$$C = -(\lambda k)^2 S(r_0) S(r_1) [K_1(kr_1)I_1(kr_0) - I_1(kr_1)K_1(kr_0)] / E \quad (8c)$$

$$D = \lambda k S(r_0) [K_0(kr_1)I_1(kr_0) + I_0(kr_1)K_1(kr_0)] / E \quad (8d)$$

$$E = \lambda k S(r_1) [I_0(kr_1)K_1(kr_1) + I_1(kr_1)K_0(kr_1)] \quad (8e)$$

Two thermal quadrupoles are needed to represent the heat transfer in the tool. The corresponding scheme is presented in Figure 2 with the exact quadrupole formulation. A reduced model with capacity and resistance is presented in Figure 3.

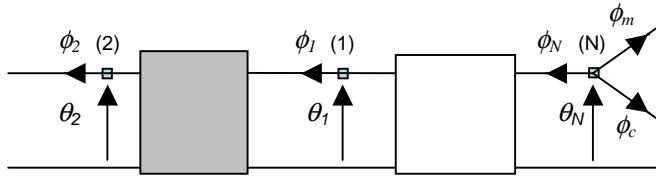


Figure 2: Exact quadrupole formulation.

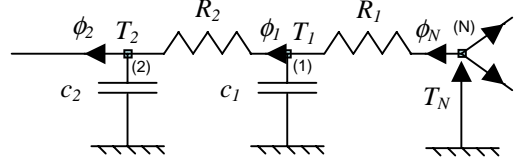


Figure 3: Approximate quadrupole formulation.

Indeed in the Laplace domain, the heat transfer in the tool between the point (N) and the point (1) -corresponding to the surfaces  $S(r_0)$  and  $S(r_1)$ - can be represented by the following matrix transfer:

$$U_N = M_1 U_1 \quad (9a)$$

The coefficients  $A_i$ ,  $B_i$ ,  $C_i$  and  $D_i$  depend on the thermophysical properties of the right side of the tool, its thickness and the Laplace variable.

For the left side of the tool that is to say between the point (1) and the point (2), corresponding to the surface  $S(r_1)$  and  $S(r_2)$ , the analogue quadrupole can be written as:

$$U_1 = M_2 U_2 \quad (9b)$$

As a consequence

$$U_N = M_1 M_2 U_2 \quad (9c)$$

### 3. TEMPERATURE AND HEAT FLUX ESTIMATION

#### 3.1 Temperature and heat flux estimation procedure

In this problem, the known quantities are the temperatures  $\theta_1$  and  $\theta_2$  (measured by thermocouples and far enough away from the tip of the tool in order not to damage the thermocouples). The four unknown are:  $\theta_N$ ,  $\phi_N$ ,  $\phi_1$ ,  $\phi_2$ .

In order to evaluate the temperature and the heat flux at the tip of the tool, the heat flux  $\phi_1$  is expressed as a function of  $\theta_1$  and  $\theta_2$ :

$$\phi_1 = C_2 \theta_2 + D_2 \phi_2 = C_2 \theta_2 + D_2 \frac{\theta_1 - A_2 \theta_2}{B_2} \quad (10)$$

The relation (10) with equation (9a) leads to the following expression of the temperature and the heat flux at the tip of the tool as functions of the two measured temperatures  $\theta_1$  and  $\theta_2$ :

$$\begin{pmatrix} \theta_N \\ \phi_N \end{pmatrix} = \frac{1}{B_2} \begin{pmatrix} A_1 B_2 + B_1 D_2 & -B_1 \\ C_1 B_2 + D_1 D_2 & -D_1 \end{pmatrix} \begin{pmatrix} \theta_1 \\ \theta_2 \end{pmatrix} \quad (11)$$

This model gives the results in the Laplace domain. A numerical algorithm (Stehfest [19] or de Hoog [10]) permits one to obtain the temperature and the heat flux as a function of time.

In order to validate the methodology previously described, numerical simulations have been performed. The geometry is the same as presented in Figure 1 and the values for the different geometrical or thermophysical parameters are summarized in Table 1 in section 2.

### 3.2 Validation of the model in the steady state case

The steady state corresponds to the limit of previous expressions (8a) (8b) (8c) (8d) when  $p$  tends to zero:

$$\lim_{p \rightarrow 0} A = 1 \qquad \lim_{p \rightarrow 0} B = \frac{\ln(r_1/r_0)}{\varepsilon_r e \lambda} \qquad \lim_{p \rightarrow 0} C = 0 \qquad \lim_{p \rightarrow 0} D = 1 \qquad (12)$$

The model is validated because for  $B$  the limit obtained corresponds to the classical result of a cylindrical thermal resistance and for  $C$  it is obvious that the calorific capacity must be zero for the steady state. Moreover the quadrupole is passive because  $AD - BC = 1$ .

### 3.3 Validation of the model in the transient case

In this section, simulations have been made with Fluent for different solicitations and estimations are made with the semi-analytical model based on the quadrupole formulation and using Bessel functions.

#### 3.3.1 Simulations

Numerical simulations with the collocated finite volume code Fluent<sup>®</sup> have been performed in order to test the model for transient heat transfer. The grid is built with particular attention, especially near the tip. All the cells have a ratio length/width (aspect ratio) between 1 and 3 and equiangle skew equal to 0. These criteria permit one to obtain high quality numerical results. The space discretization uses a power law scheme which computes accurately the diffusion. The time integration uses a second order scheme. Moreover, several other simulations are performed in order to prove that the results are independent of the grid (grid with  $13700 \times 4$  cells).

The temperature of the isothermal surface  $S(r_2)$  is imposed at 300 K, the temperature of the tip is a function of time  $T_0(r=r_0, t)$ . The transient temperature is then calculated with a step  $\Delta t = 5 \cdot 10^{-2}$  s (this time step is short enough compared to the characteristic time of the tool). For each time step, the temperature  $T_1$  of a point located on the bisector of the tool for the medium radius  $r_1$  is saved. Then the measured temperature  $T_1$  and the temperature  $T_2$  are introduced in the equation (11). The temperature and the heat flux of the tip could be evaluated. The results obtained are then compared with the input temperature  $T_0$  in Fluent<sup>®</sup>.

Let us now consider the reduced time and the reduced temperature defined by:

$$t^* = \frac{\alpha t}{r_2^2} \qquad (13a)$$

$$T^* = \frac{T - T_{ext}}{T_0 - T_{ext}} \qquad (13b)$$

#### 3.3.2 Estimation in the case of a Heaviside temperature solicitation

In this test case, the temperature solicitation on the tip is a Heaviside function that is to say:

$$T_0^* = T^*(t \geq 0, r = r_0) = 1. \qquad (14)$$

The results obtained with Fluent<sup>®</sup> (Input Temperature) and the analytical model (Estimated Temperature) following the procedure described in the sections 3.1 and 3.3.1 are plotted in figure 4.

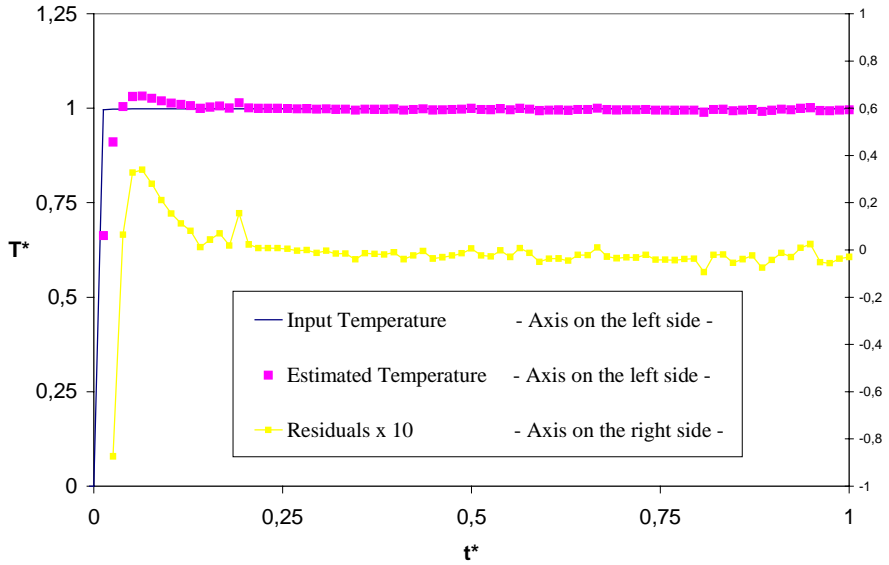


Figure 4: Comparison between the input temperature at the tip in the direct model (simulations with Fluent®) and the estimated temperature (from equation 11) for Heaviside solicitation.

The transient temperatures present the same shape. The major errors are encountered for short times but this can be easily explained by physical considerations. Indeed for  $t^* = 0$ , the Heaviside solicitation corresponds to an infinite heat flux and there is a temperature jump (mathematical discontinuity). Let us consider a more realistic physical solicitation for the thermal behaviour during the turning process.

### 3.3.3 Estimation in the case of an exponential temperature solicitation

The transient temperature solicitation is represented now by an exponential function:

$$T_0^* = T^*(t, r = r_0) = \frac{T - T_{ext}}{T_0 - T_{ext}} = 1 - \exp(-2t). \quad (15)$$

The characteristic time of heating is about  $0.5 s$ , it takes about  $3 s$  to reach the final temperature  $T_0$  that corresponds to the experimental conditions. The results are presented in Figure 5.

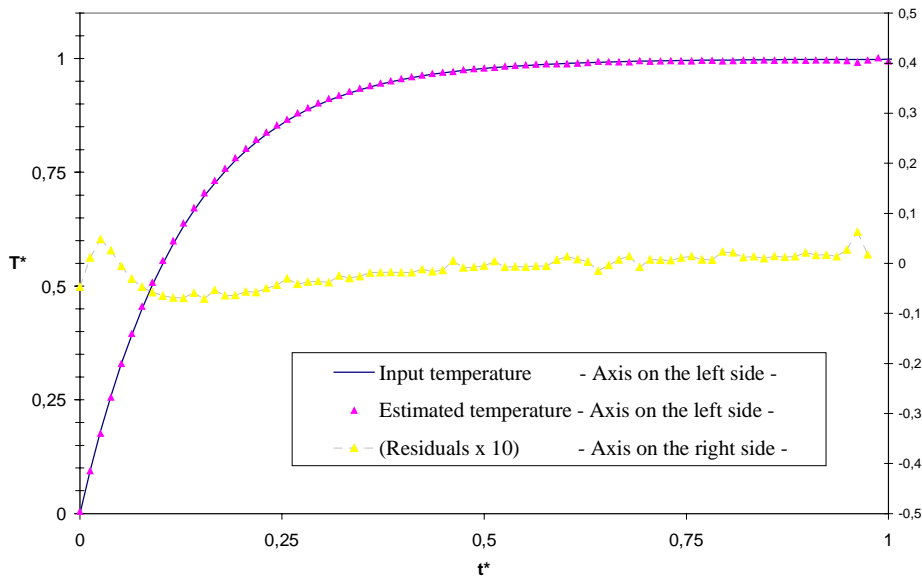


Figure 5: Comparison between the input temperature at the tip in the direct model (simulations with Fluent®) and the estimated temperature (from equation 11) for exponential solicitation.

A very good agreement between the results with Fluent® and with the analytical model is obtained. The errors between the transient estimated temperature and the input temperature are less than 3 %. The predictive model based on the quadrupole formulation is thus validated.

### 3.3.4 Estimation in the case of noisy data

Experimental measurements are always corrupted by noise. The causes of the noise are for instance perturbations at the thermocouples. In the case of thermal measurements during the turning process, perturbations are essentially due to the mechanical vibrations. In order to test the analytical predictive model in a more realistic case, noise is added to the transient temperature. The thermal behaviour of the tool is presented in Figure 6 and the analytical model predicts accurately the temperature of the tip of the tool.

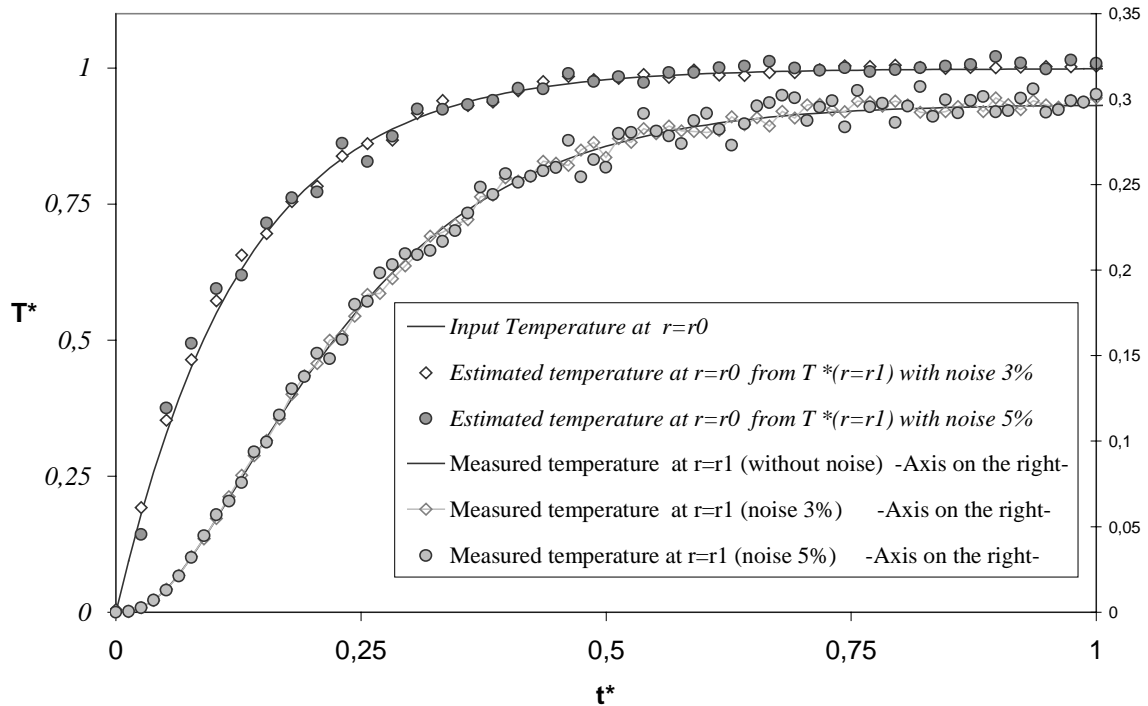


Figure 6: Measured temperature at  $r=r1$  (with noise) and estimated temperature at the tip of the tool.

## 4. CONCLUSION

The interrelationships among the transient temperature and the heat flux at the tool's tip and the two measured temperatures are established from using an inverse approach based on an adequate and efficient quadrupole formulation. It provides a new and promising method to easily estimate the transient temperature at the tip of a turning tool in order to prevent and to avoid the damage or the breaking of the tool. The approach proposed here can be used with application to an adaptive control of the cutting temperature. Simulations for different temperature profiles are performed (Heaviside, exponential or noised solicitations). The results obtained with our predictive analytical model are in good agreement with those obtained with Fluent®. Future work in this study is to perform measurements.

## REFERENCES

1. H. Ay and W.J. Yang, Heat transfer and life of metal cutting tools in turning. *Exp. Heat Transfer* (1994) **41**, 203-216.
2. H. Ay and W.J. Yang, Dynamics of cutting tool temperatures during cutting. *Int. J. Heat Mass Transfer* (1998) **41**, 613-623.
3. C. Barlier, C. Lescalier and A. Moisan, Continuous flank wear measurement of turning tools by integrated micro-thermocouple, 47<sup>th</sup> Annal of CIRP Tianjin August 1997- 46/1, 35-38.
4. J. L. Battaglia and J.C. Batsale, Estimation of heat flux and temperature in a tool during turning. *Inv. Prob. in Eng.*, (2000), 1-23.
5. J. L. Battaglia *et al*, Solving an inverse heat conduction problem using a non-integer identified model. *Int. J. Heat Mass Transfer*, (2001), 2671-2680.
6. J. V. Beck, and K. J. Arnold, *Parameter Estimation in Engineering and Science*, John Wiley & Sons, New-York, 1977 .
7. G. Boothroyd, Temperatures in orthogonal metal cutting. *Proceedings of the Institution of the Mechanical Engineers* (1963) 789-802.
8. G. Boothroyd and W.A. Knight, *Fundamentals of Machining and Machine Tools*, Marcel Dekker, New York, 1989.
9. N. H. Cook, *Prediction of Tool Life and Optimal Machining Conditions*, Symposium on Cutting Tools and Wear related Phenomena, Lausanne, Switzerland, 1979.
10. F. R. De Hoog, J. H. Knight and A. N. Stokes, Quotient difference method with accelerated convergence for the continued fraction expansion". *SIAM J. Sci. Stat. Comput.* (1982) **3**, 357-366.
11. A. Degiovanni, Conduction dans un mur multicouche avec sources: extension de la notion de quadripôle, *Int. J. Heat Mass Transfer* (1988) **31**, 553-557.
12. S.P. Jaspers, J.H. Dautzenberg, and D.A. Taminiau, Temperature measurement in orthogonal metal cutting, *Int. J. Adv. Manuf. Technol* (1998) 7-12.
13. P. Kwon T. Schiemann and R. Kountanya, An inverse estimation scheme to measure steady state tool-chip interface temperatures using an infrared camera. *Machine Tools and Manufacture* (2001) **41**, 1015-1030.
14. M. Lazard and P. Corvisier, Modeling of a tool during turning. Analytical prediction of the temperature and of the heat flux at the tool's tip. *Applied Thermal Engineering*, (2004) **24**, 839-849.
15. S. Lei, Y.C. Shin and P.P. Incropera, Thermal mechanical modelling of orthogonal machining process by finite element analysis. *International Journal of Machine Tools and Manufacture* (1999) **39**, 731-750.
16. D. Maillet, S. André, J.C. Batsale, A. Degiovanni and C. Moyne, *Thermal Quadrupoles: An Efficient Method for Solving the Heat Equation through Integral Transforms*, John Wiley and Sons, New York, 2000.
17. P.L.B. Oxley, Modelling machining processes with a view to their optimization and to the adaptive control of metal cutting machine tools, *Robotic and Computer Integrated Manufacturing* (1988) 103-119.
18. M.C. Shaw, *Metal Cutting Principles*, Oxford University Press, Oxford, 1989.
19. H. Stehfest, Remarks on algorithm 368. Numerical inversion of Laplace transform. *Com. A.C.M.* 624, (1970) **13**, 47-49.